A robust and unique iron(II) mosaic-like MOF

Estefania Fernandez-Bartolome, José Santos, Saeed Khodabakhshi, Laura J. McCormick, Simon J. Teat, Cristina Saenz de Pipaon, Jose R. Galan-Mascaró's, Nazario Martín and Jose Sanchez Costa
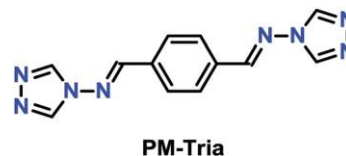
A novel extended triazole-based ligand (PM-Tria) has been synthesized and an unprecedented MOF 3D has serendipitously been formed by assembling iron(II), PM-Tria ligand and fluoride anions. This MOF contains a perfectly linear one-dimensional $\{Fe(II)-F\}_n$ bridging chain that shows an antiferromagnetic behaviour. Furthermore, the structure is compared with a 14th century mosaic found in the Alhambra Palace in Granada showing a surprising symmetry resemblance.

Coordination polymers, or most often called metal–organic frameworks (MOF),[1] are currently a hot topic in science. As an illustrative example of their relevance, in 2017 it was estimated that 6000 novel MOFs are published each year.[2] This vast interest derives from the fact that MOFs show a wide variety of potential applications, which include gas uptake, catalysis, luminescence, electrical conductivity or biotechnology among many others. All these properties arise from their intrinsic porosity and versatility.[3–6] In fact, MOFs are extended molecular materials formed by metal ions or metal ion clusters bridged by relatively long organic ligands, thus creating size-tunable structural voids to absorb guest molecules and act as highly specific molecular vessels with different absorption capabilities.[7,8] MOFs can also display different reactivities towards targeted molecules based on the different electronic environments created within the cavities. In addition, the modular nature of MOFs (via the combination of inorganic and organic components) makes them ideally suited to chemical manipulation, aiming at fine-tuning their structure and function.[9] Nevertheless, obtaining novel compositions or novel synthetic methods,[10,11] with the aim of obtaining targeted specific properties for their ultimate technological application, is still a real challenge. Despite the fact that the colossal database of novel MOFs has enabled the development of novel synthetic tools and progress of the rational design vs. the serendipitous assembly, this second method's randomness is still offering us beautiful surprises every now and then (Scheme 1).

In this manuscript, a novel Fe(II) MOF is described by assembling Fe(II), PM-Tria ligands and fluoride anions. The 1D Fe(II)–F chain exhibits a perfect linearity on its growing-mode, which allows the expansion of the structure in the third dimension by means of the PM-Tria ligands. The magnetic behaviour of this material is also reported. Furthermore, this molecular architecture astonishingly resembles a 14th Century Islamic mosaic located at the Alhambra Palace in Granada (Spain) that shows beautiful symmetric patterns.[12] With the aim of obtaining large cavities coupled to metal centers that may be susceptible to achieve one of the most fascinating molecular switchable processes, the so-called spin crossover,[13,14] we have synthesized a novel bridging triazole-based ligand, namely [1,4-phenylene(methanylylidene)]-4H-1,2,4-triazol-4-amine (PM-Tria). The pure PM-Tria ligand is prepared from terephthalaldehyde and 4-amino-1,2,4-triazole through a straightforward Schiff-base condensation reaction, with nearly quantitative yield (see the ESI†).

Reaction of 1 equivalent of $Fe(BF_4)_2$ with 1.33 equivalents of PM-Tria in ethanol at 140 1C in a pressure vessel provides, after four days, red cubic crystalline materials with $\{[Fe(PM-Tria)_2(\mu_2-F)][BF_4]\}_n$ (1) formulation in moderate yield (20%).

[a] IMDEA Nanociencia, C/ Faraday 9, Ciudad Universitaria de Cantoblanco, 28049, Madrid, Spain. E-mail: jose.sanchezcosta@imdea.org

[b] Advanced Light Source, Berkeley Laboratory, 1, Cyclotron Road, CA 94720, Berkeley, USA

[c] Institute of Chemical Research of Catalonia (ICIQ), The Barcelona Institute of Science and Technology (BIST), Avda. Països Catalans, 16, 43007, Tarragona, Spain

[d] ICREA, Pg. Lluís Companys, 23, 08010, Barcelona, Spain

[e] Facultad de Ciencias Químicas, Universidad Complutense de Madrid, Madrid, 28040, Spain

† Electronic supplementary information (ESI) available. CCDC 1825247. For ESI and crystallographic data in CIF or other electronic format see DOI: 10.1039/c8cc01561a

PM-Tria

Scheme 1 The PM-Tria ligand [1,4-phenylenebis(methanylylidene)]bis-(4H-1,2,4-triazol-4-amine).

The fluoride ligand is in situ generated by the decomposition of the BF_4^- counterion of the starting Fe(II) salt (see the ESI,† Section 3, for more details).

Decomposition of the tetrafluoroborate anion, through hydrolysis or fluoride abstraction, has been long known as a potential fluoride source in coordination compounds.[15,16] After this observation, an alternative reaction has been performed by adding FeF_2 salt in combination with $Fe(BF_4)_2$ and PM-Tria in a 1 : 1 : 2.5 molar ratio. After four days, red crystalline cubic materials similar to those previously described are observed, but in a higher reaction yield of 38% (see the ESI† for further details).

Single-crystal X-ray diffraction of 1 was examined at 100 K. Compound 1 crystallizes in a tetragonal space group P4/ncc. The asymmetric unit contains three PM-Tria ligands and three crystallographic inequivalent iron(II) metal centers that are compensated by three BF_4^- and three F^- counterions. Details of the structure solution and refinement are summarized in Section 7 of the ESI,† and selected bond lengths and angles are given in Tables S2–S4 and Fig. S10 and S11 (ESI†). As expected for an iron(II) cation, the metal center shows an octahedral environment.[17,18] Fe(II) is coordinated by four nitrogen atoms (belonging to four triazole-based PM-Tria ligands) placed at the equatorial sites and two fluoride ions acting as coordinating m_2 ligands at the axial positions.

Every Fe(II) center is connected to four neighbouring Fe(II) via four bridging PM-Tria ligands (Fig. 1c). Surprisingly, triazole acts uniformly with a monodentate m_1 bridging character instead of the well-known bidentate nature of this kind of ligand with Fe(II) metal centers.[19] The three-dimensional structure is expanded along the quasi-perfect one-dimensional $\{Fe(II)-F\}_n$ polymeric unit (Fig. 1a, 2a and b). The average Fe–X = 2.1 Å bond length, X being N and F donor atoms, is an effective indication that the metal center is in its high-spin (HS) electronic configuration at the given temperature (Table S2, ESI†). This observation is also confirmed by the magnetic measurements (see below in this communication).

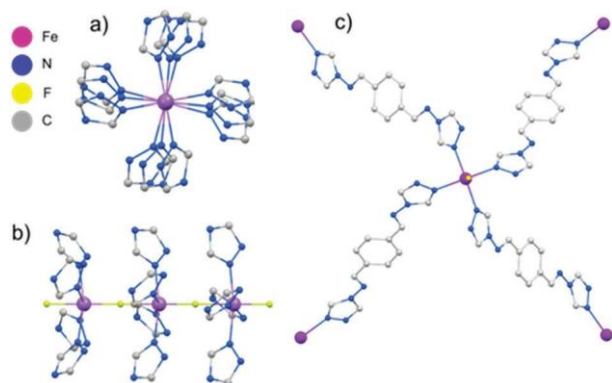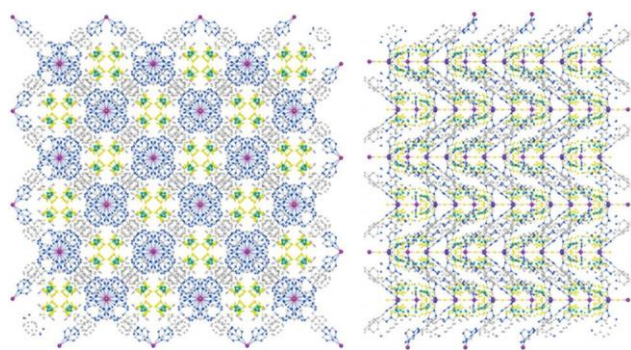The crystal packing of 1 along the c-axis shows that the polymeric one-dimensional chains are packed parallel to the

Fig. 2 (a) The c axis view of 1 revealing the cavities contained by the structure. (b) The representation along the b axis evidencing the collapsed character of the structure.

c-axis with an interchain distance between iron centers of 19.94 Å. Interestingly, the PM-Tria ligands are tilted 35.711 with relative to the Fe–F–Fe chain (Fig. 2b).

These ligands display strong supramolecular interactions between them, evidenced by short ring to ring contacts (the shortest being 3.337 Å, see Fig. S10, ESI†), which allows in turn building a robust extended MOF. Moreover, it is worth mentioning that the tetrafluoroborate counterions required for a charge balance weakly interact with the PM-Tria ligands. At the same time, these interactions reinforce the structural stability of the crystals in the three dimensions (Fig. 2a, 3 and Fig. S10, ESI†).

As expected for a collapsed framework (see Fig. 2b) the Brunauer–Emmett–Teller (BET) surface area is low, concretely, 6.7 m^2 g^{-1}. According to the structural analysis, this accounts for a solvent-accessible volume of 640 $Å^3$ and a molecular surface area of 755 $Å^2$ (see Fig. S13, ESI,† for further details).

The infrared spectrum of 1 shows the characteristic vibrational modes of the three components, i.e. the PM-Tria ligand and the BF_4^- and the F^- counterions (Fig. S3–S6, ESI†). X-ray powder diffraction of the different crystalline samples synthetized by both strategies has been compared with the theoretically obtained single-crystal X-ray diffraction of 1, affording a superimposed spectrum.
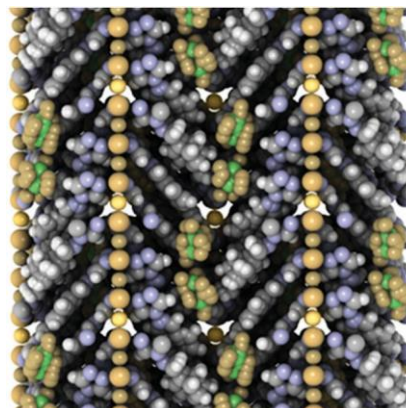

Fig. 1 MERCURY view of 1 (hydrogen atoms have been removed for clarity). (a) c view of a trimeric unit. (b) b view of an Fe(II)···F···Fe(II) trimeric unit. (c) A segment of 1 illustrating the metallic connection along the c axis via PM-Tria ligands.

Fig. 3 iRASPA[20] representation of 1 along the a axis. This illustration shows how perfect the one-dimensional chains are, and the way the counterions fill in the empty space in the network allowing the growth of the crystalline material.

The thermogravimetric study of 1 confirms the presence of solvent molecules from the synthesis (approximately 0.5 molecules of ethanol and 1.5 water molecules per unit cell). In addition to this information, at around 225 1C, an irreversible weight loss corresponding to the decomposition process of the MOF (Fig. S7, ESI†) is observed.

The magnetic properties of 1 were determined in the 2–300 K temperature range under a constant field of 1 T and the data are summarized in Fig. 4. The value of $\chi_M T$ at room temperature is 2.5 cm^3 K mol^{-1}, slightly lower than the spin-only value expected for a magnetically diluted S = 2 sample (of 3 cm^3 K mol^{-1}). This confirms the HS state of the Fe(II) centers and suggests the presence of antiferromagnetic coupling between spin carriers. Indeed, the $\chi_M T$ product decreases when the temperature is decreased (Fig. 4, square dots). The χ_M vs. T plot (Fig. 4, triangle dots) shows a maximum around 50 K which is also a signature of dominant antiferromagnetic interactions. The high temperature regime can be fitted to a Curie–Weiss law (Fig. S15, ESI†), with parameters C = 3.85 cm^3 K mol^{-1} (g = 2.24) and $y = -10.6$ K. However, the low temperature data deviate significantly from this model, with the appearance of a Curie tail that indicates the presence of a paramagnetic contribution. Since interchain distances are one order of magnitude longer than the intrachain ones, we can consider in a first approximation that only the fluoride bridges are effective magnetic super-exchange pathways. Thus, we modeled the magnetic data to the analytical expression for an infinite chain of classical spins, as derived by Fisher from the exchange Hamiltonian (see the ESI† for equation details).[21] This model satisfactorily reproduces the data in all the temperature range, with parameters S = 2, g = 2.12, J = −16 cm^{-1} and C_P = 0.03 cm^3 K mol^{-1} (see red and blue lines in Fig. 4). Such small paramagnetic contribution corresponds approximately to 1% of the total Fe(II) content. It is probably related to the terminal metal centres, since the actual chains (and crystals) are not infinite as the model supposes. The antiferromagnetic nature of the fluoride-bridged chains is also consistent with their geometry. The Fe–F–Fe bridges of 1801 favour an orbital overlap between semi-occupied metal orbitals carrying unpaired spins, stabilizing a ground state with unparalleled spin alignment.[16]

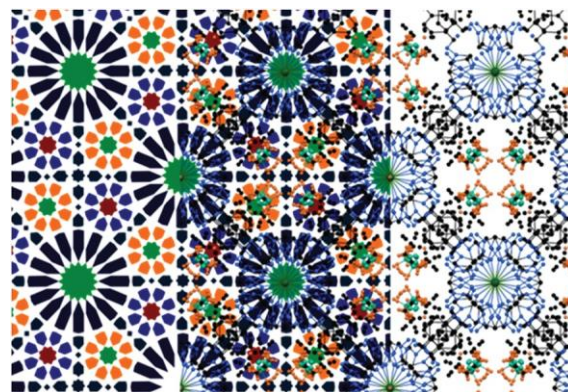A mosaic is defined as a design made with small pieces of ceramic, glass, stones or other objects. These can either be

Fig. 5 On the left we see the Islamic mosaic found at the Alhambra Palace of Granada. On the right is an illustration of 1 along its c-axis. In the middle is a superposition of the two pictures.

organized in exact geometric shapes or created from more haphazard and broken pieces. There has been an enormous amount of research on mosaic tilings worldwide, and they are a source of many teaching subjects in mathematics and art. Probably, the Dutch M. C. Escher is one of the most recognized artists inspired by these pieces of arts.

He was greatly surprised by Islamic art after visiting the Alhambra Palace in Granada (Spain) in 1922 and 1936. Later, in 1958, he published a book titled 'Regular Division of the Plane', in which he described the systematic build-up of mathematical bridges. Today the Escher techniques are well known to create tiles that, by applying geometric movements, may be used to produce a variety of mosaics. What we have found for 1 is that the view generated along the c axis almost perfectly fits with an Islamic mosaic found at the Alhambra Palace (see Fig. 5 and Fig. S15, ESI†). This genuine tessellation found for 1 mainly arises from an unusual rotation of the central metal equatorial coordination plane along the one-dimensional direction. In particular, the rotation from Fe(1) to Fe(2) planes is 16.031 and from Fe(2) to Fe(3) is 9.231. The total rotation from Fe(1) to Fe(3) is equal to 25.261 (see Fig. S11, ESI†). Remarkably, the tetrafluoroborate counterions fill the space that in the mosaic is occupied by an octagram.

In summary, a novel extended triazole-based ligand (PM-Tria) has provided a very promising entry into a MOF 3D architecture with Fe(II)–F chains which exhibits a perfect linearity on its growing-mode. The magnetic study of this material confirms an antiferromagnetic 1D behaviour. Finally, this molecular architecture is compared with an XIV century Islamic mosaic found in the Alhambra Palace in Granada (Spain) showing a surprising and beautiful resemblance.

Fig. 4 χ_M vs. T (triangle dots for experimental data and the red line for a fitting curve) and $\chi_M T$ vs. T (square dots and blue line) plots.

Conflicts of interest

There are no conflicts to declare.

Notes and references

1 H. Furukawa, K. E. Cordova, M. O'Keeffe and O. M. Yaghi, Science, 2013, 341, 1230444.
2 MOFs find a use | Feature | Chemistry World, https://www.chemistryworld.com/feature/mofs-find-a-use/2500508.article, accessed 5 February 2018.
3 H. Deng, S. Grunder, K. E. Cordova, C. Valente, H. Furukawa, M. Hmadeh, F. Gandara, A. C. Whalley, Z. Liu, S. Asahina, H. Kazumori, M. O'Keeffe, O. Terasaki, J. F. Stoddart and O. M. Yaghi, Science, 2012, 336, 1018–1023.
4 N. Zhang, B. Zhu, F. Peng, X. Yu, Y. Jia, J. Wang, L. Kong, Z. Jin, T. Luo and J. Liu, Chem. Commun., 2014, 50, 7686.
5 S. Qiu, M. Xue and G. Zhu, Chem. Soc. Rev., 2014, 43, 6116–6140.
6 M. Zhao, K. Deng, L. He, Y. Liu, G. Li, H. Zhao and Z. Tang, J. Am. Chem. Soc., 2014, 136, 1738–1741.
7 J. A. Mason, J. Oktawiec, M. K. Taylor, M. R. Hudson, J. Rodriguez, J. E. Bachman, M. I. Gonzalez, A. Cervellino, A. Guagliardi, C. M. Brown, P. L. Llewellyn, N. Masciocchi and J. R. Long, Nature, 2015, 527, 357–361.
8 E. D. Bloch, W. L. Queen, R. Krishna, J. M. Zadrozny, C. M. Brown and J. R. Long, Science, 2012, 335, 1606–1610.
9 J. Lee, O. K. Farha, J. Roberts, K. A. Scheidt, S. T. Nguyen and J. T. Hupp, Chem. Soc. Rev., 2009, 38, 1450.
10 P. J. Waller, F. Gándara and O. M. Yaghi, Acc. Chem. Res., 2015, 48, 3053–3063.
11 J. Jiang, Y. Zhao and O. M. Yaghi, J. Am. Chem. Soc., 2016, 138, 3255–3265.
12 B. L. Bodner, Proc. Bridg. Math. Music. Art, Archit. Cult., 2013, 225–232.
13 G. Molnár, S. Rat, L. Salmon, W. Nicolazzi and A. Bousseksou, Adv. Mater., 2017, 17003862.
14 J. S. Costa, S. Rodríguez-Jiménez, G. A. Craig, B. Barth, C. M. Beavers, S. J. Teat and G. Aromí, J. Am. Chem. Soc., 2014, 136, 3869–3874.
15 S. Dammers, T. P. Zimmermann, S. Walleck, A. Stammler, H. Bögge, E. Bill and T. Glaser, Inorg. Chem., 2017, 56, 1779–1782.
16 K. S. Pedersen, M. A. Sørensen and J. Bendix, Coord. Chem. Rev., 2015, 299, 1–21.
17 G. A. Craig, J. S. Costa, O. Roubeau, S. J. Teat and G. Aromí, Chem. – Eur. J., 2012, 18, 11703–11715.
18 Y. Garcia, V. Niel, M. C. Muñoz and J. A. Real, in Spin Crossover in Transition Metal Compounds I, ed. P. Gutlich and H. A. Goodwin, Springer, 2004, vol. 233, pp. 229–257.
19 O. Roubeau, Chem. – Eur. J., 2012, 18, 15230–15244.
20 D. Dubbeldam, S. Calero and T. J. H. Vlugt, Mol. Simul., 2018, 7022, 1–24.
21 O. Kahn, Berichte der Bunsengesellschaft für Phys. Chemie, 1994, 98, 1208.